Origin of breast cancer metastasis

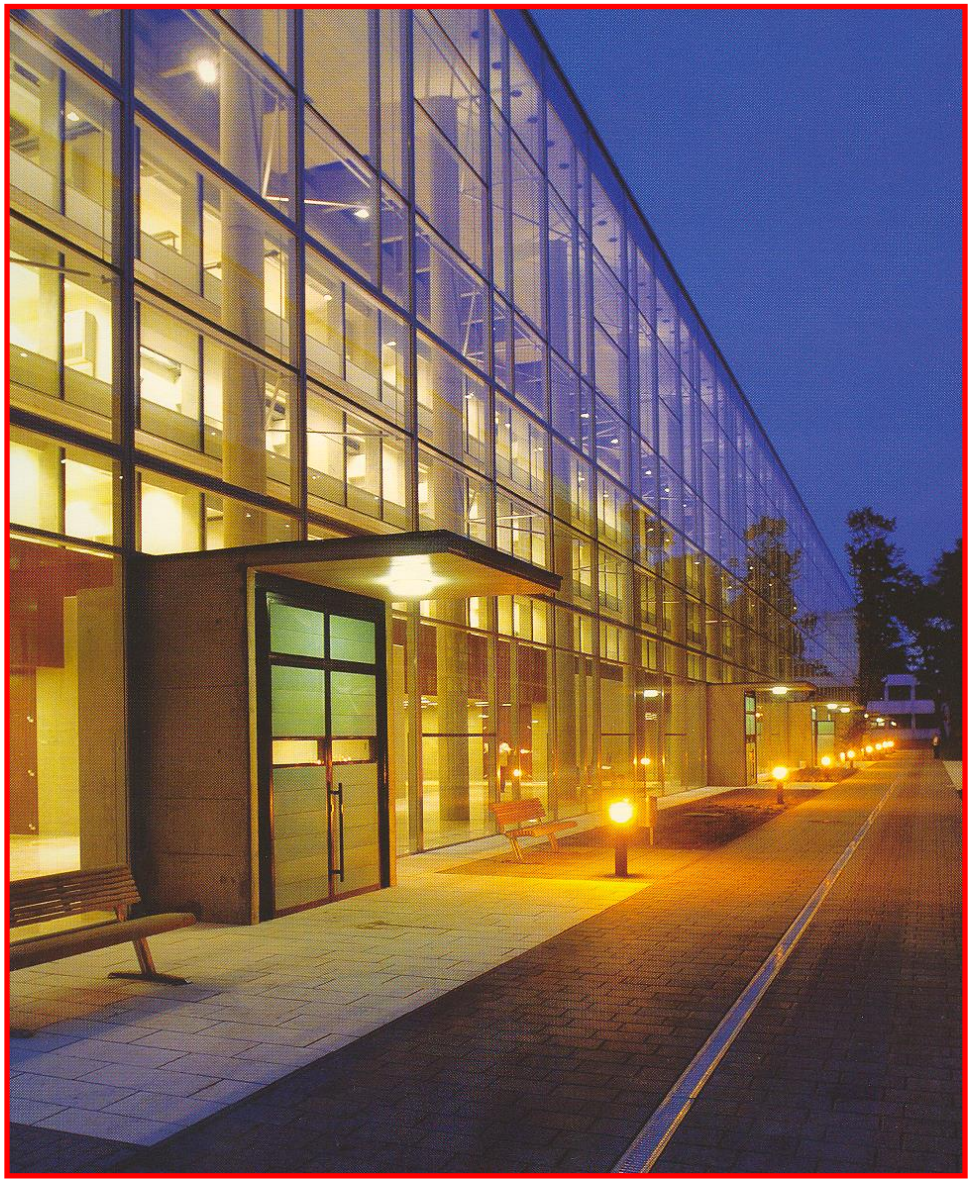

Gaspar Banfalvi

University of Debrecen

Department of Biotechnology

Aim

Abdominal organs are frequent targets of cancer cell invasion, but less known for their metastatic potential to other organs, particularly to breast.

Our aim was to follow the common steps of abdominal tumor cell progression in rats upon *i.p.* administration, subrenal or subhepatic implantation of solid tumor and leukemia cells and mimicking their migration with inorganic colloidal particles.

The work was started at the Univerity of Szeged and continued at the University of Debrecen

Tumor diagnostics – Szeged University

^{113m}Indium chloride, colloid, and macroaggregate prepared in 1970

Conclusion: after *i.v.* administration

In-chloride: acidic solution, circulated with blood could be used in small quantities (0.1-0.2 ml) (but not recommended)

In-colloid: accumulated in the liver (recommended and used)

In-Fe-macroaggregate: caused microembolization in the lungs of rats (the particle size was unreliable and large particles coukd cause death, thus it could not be used in human diagnostics (counterindicated)

^{113m}Indium macroaggregate formation

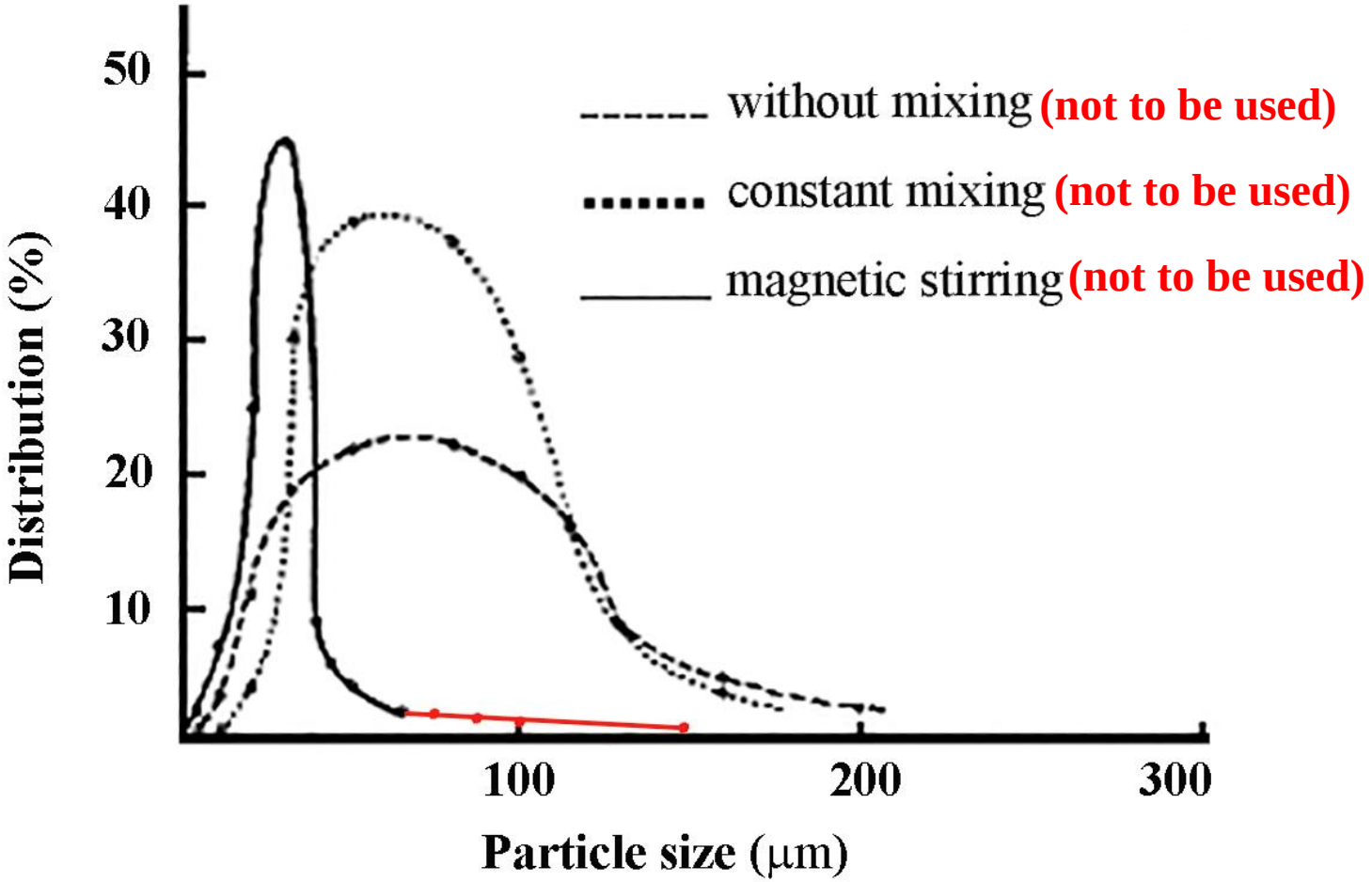

…… life threatening particle size

Organ distribution of *i.v.* administered ^{113m}In-colloid particles in rats

- **Liver** **85-90 % (Kupffer cells)**
- **Spleen** **3-5 %**
- **Bone marrow** **5-10 %**

Primary lymphoid organs:

- bone marrow, and the thymus

Secondary lymphoid organs:

- lymph nodes, tonsils, spleen, and
- "MALT" (mucosa- associated lymphoid tissue, Kupffer cells of the liver, microglia of the central nervous system

Reticuloendothelial system (RES) = Mononuclear phagocytic system and **lymphoreticular system**

Heart scintigraphy with $^{113m}InCl_3$ solution

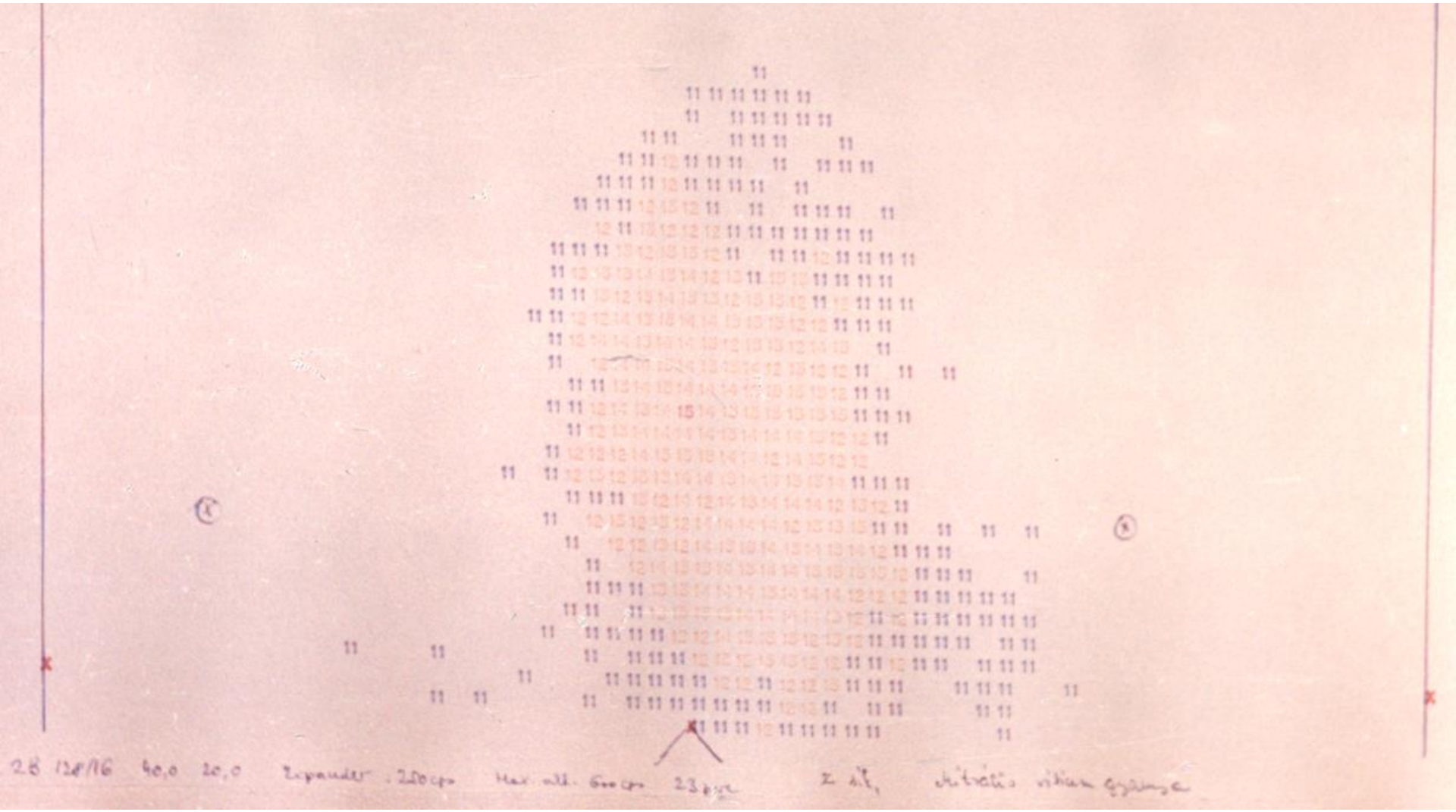

Banfalvi, G. Production of [1] ^{13m}In-preparations suitable for diagnosis
PhD dissertation , 1971, University of Szeged, 1st Department of Medicine

Normal liver scintigram

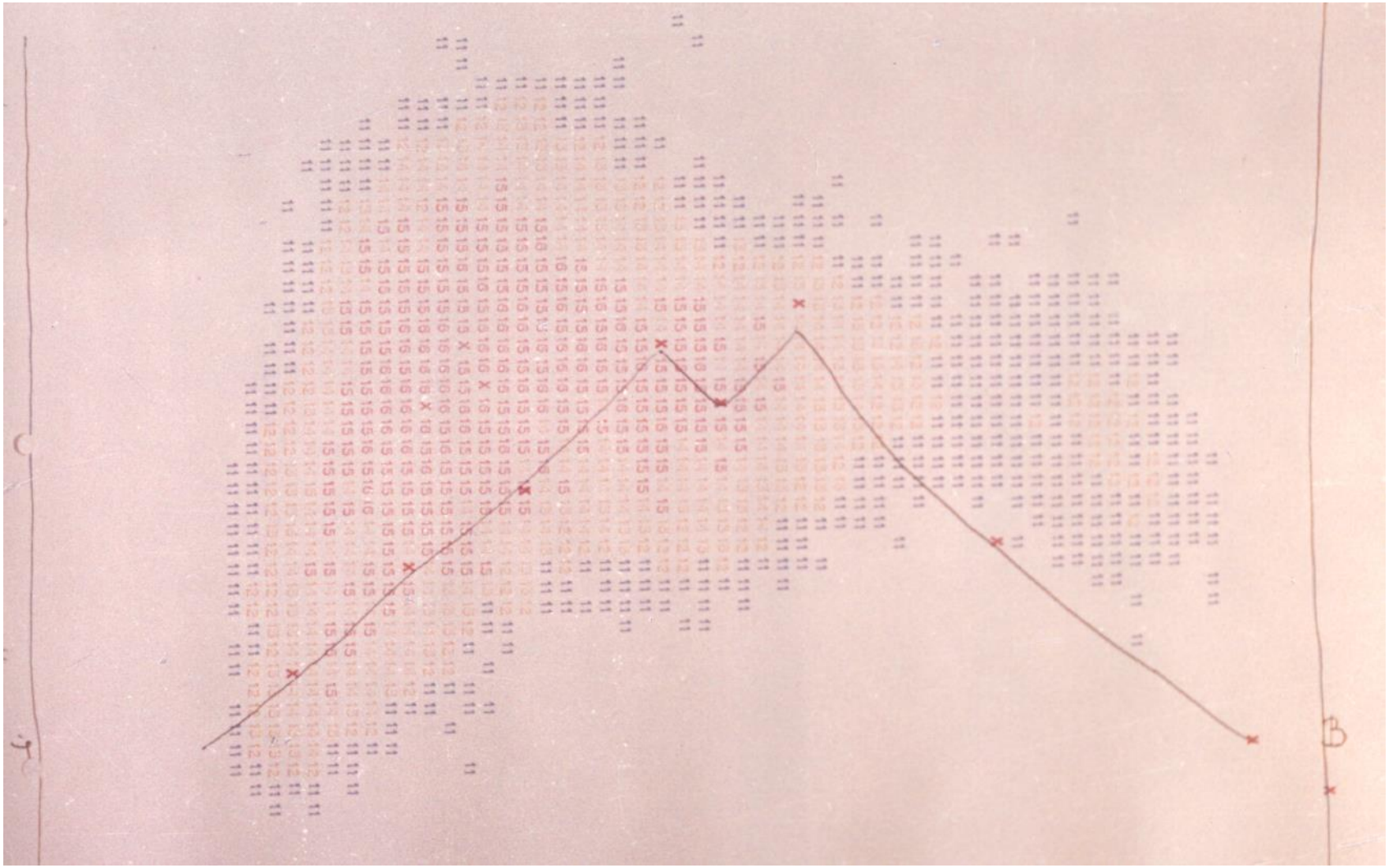

Bánfalvi , G. Banfalvi, G. Production of $^{1\ 13m}$In-colloid suitable for liver scintigraphy PhD dissertation, 1971 Szeged, Department of Internal Medicine

Hepatomegaly

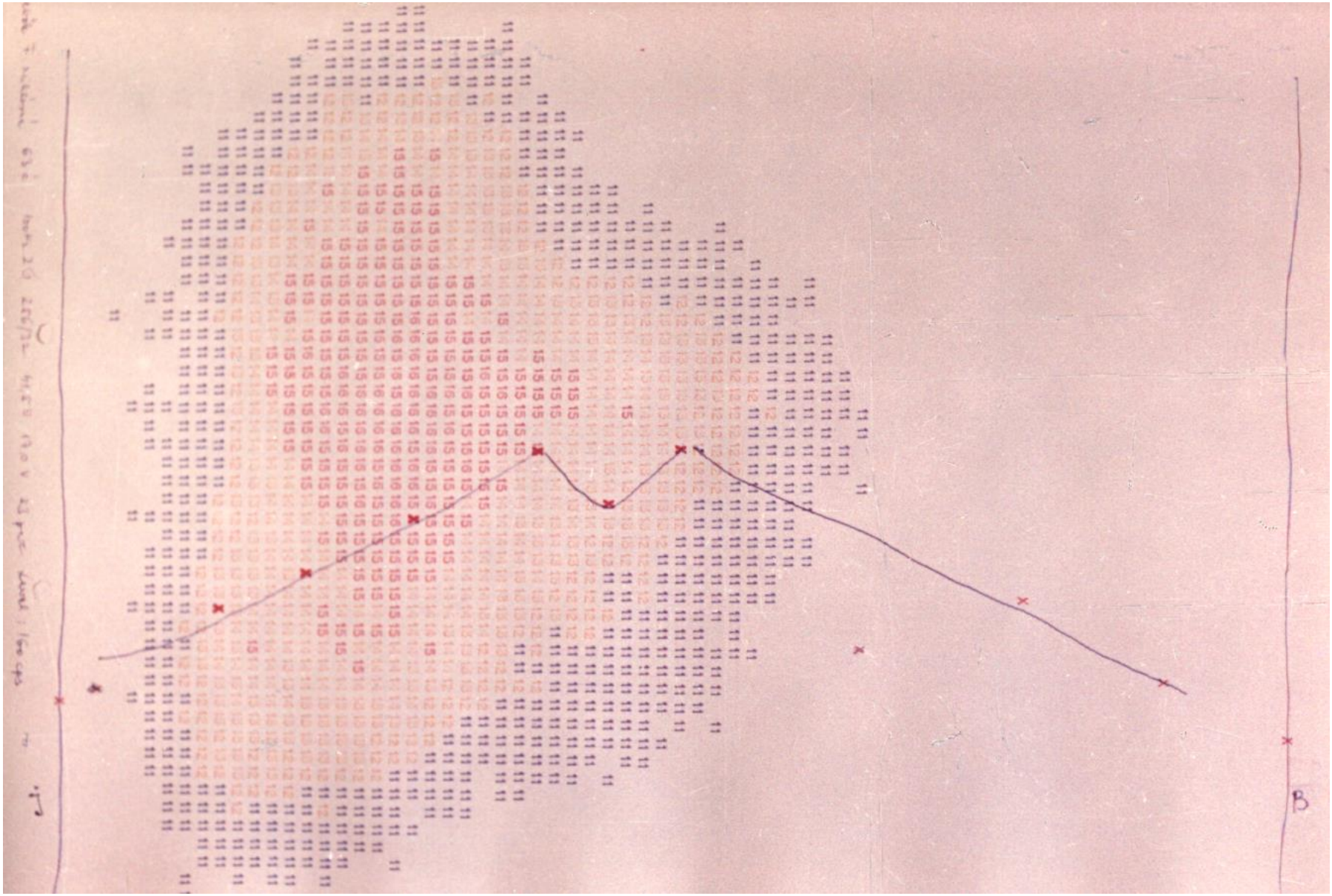

Tumor in the liver

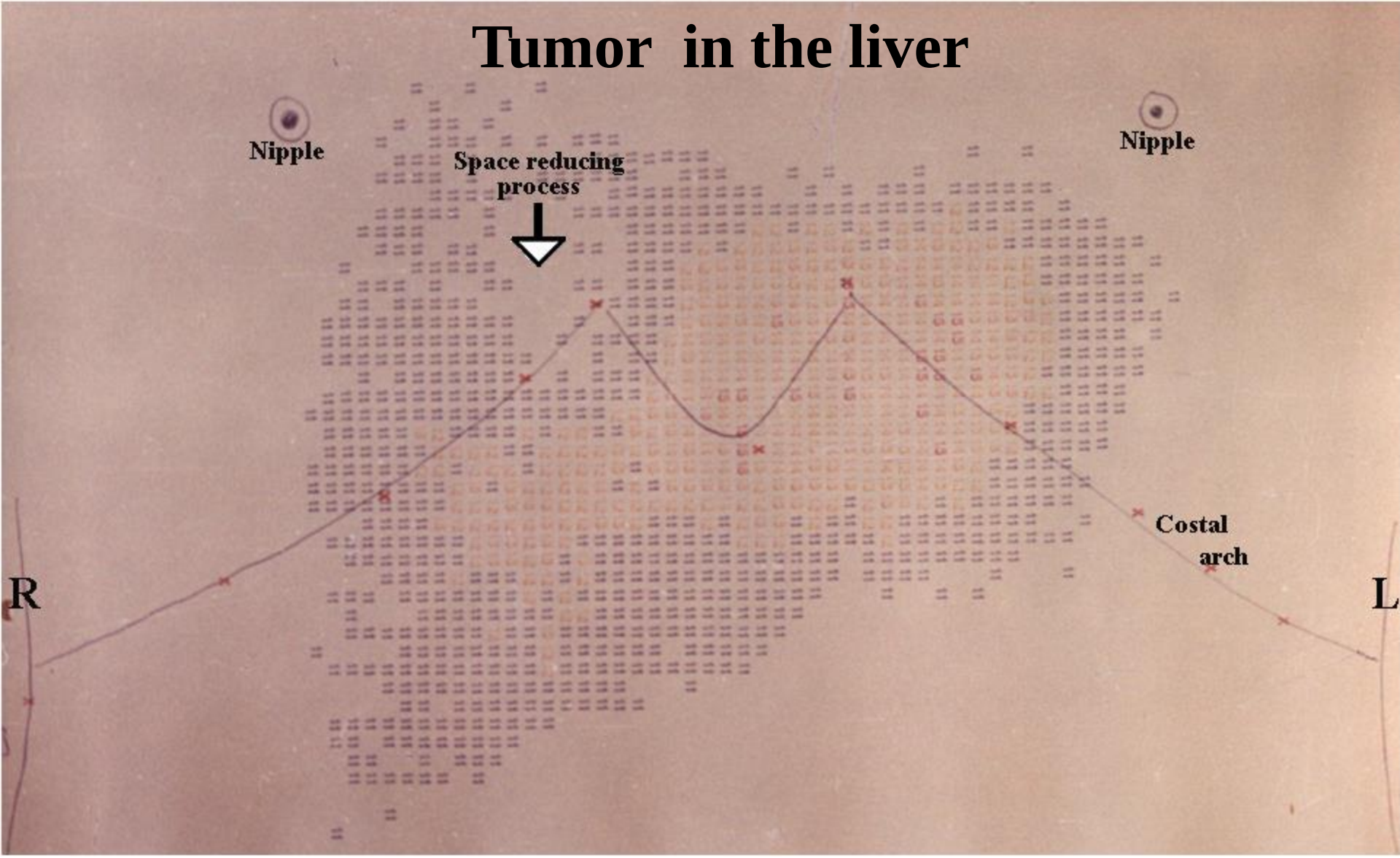

Human liver scintigraphy using ^{113}In-colloid. In the upper right corner of the liver there was no colloid accumulation indicative of an abnormal process. Medical University, Szeged. Ist Department of Internal Medicine (^{113}In-colloid prepared by G. Banfalvi in 1970).

Colloid (nano) particles in the organism:

Similar to ultrafine particles,
nanoparticles are sized between 1 and 100 nanometers

Colloid particles are between 1 nm and 10 micrometers
- viruses,
- bacteria,
- yeast cells,
- **cancer cells** (cancer cells often are different in their sizes and shapes)
- cell remnants,
- **carbon particles** (e.g. India ink)
- thin fibrous crystals of asbestos

Foerign particles are attacked by white blood cells:
- granulocytes,
- monocytes,
- lymhocytes)

Debrecen cancer cells >

Tumor biology in Debrecen

Primer cells, cell culture, cell line

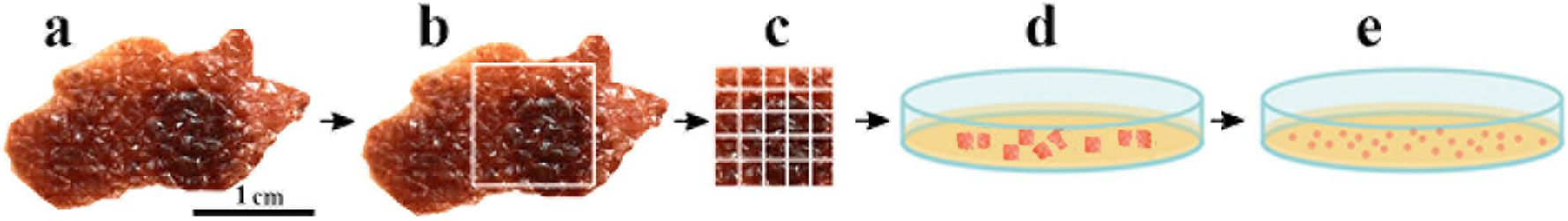

Clinical isolate (melanoma) → Part of tumor → Sliced tumor (2x2x2 mm) → Elastase digestion → Cell culture

Melanoma obtained from Department of Dermatology
Tumor cell line: *Melanoma Debreceniensis* (*Me/D*e) (2008)

Establishment of He/De, Ne/De, My1/De, My2/De, Me/De cell lines

Syngenic and xenograft tumor models

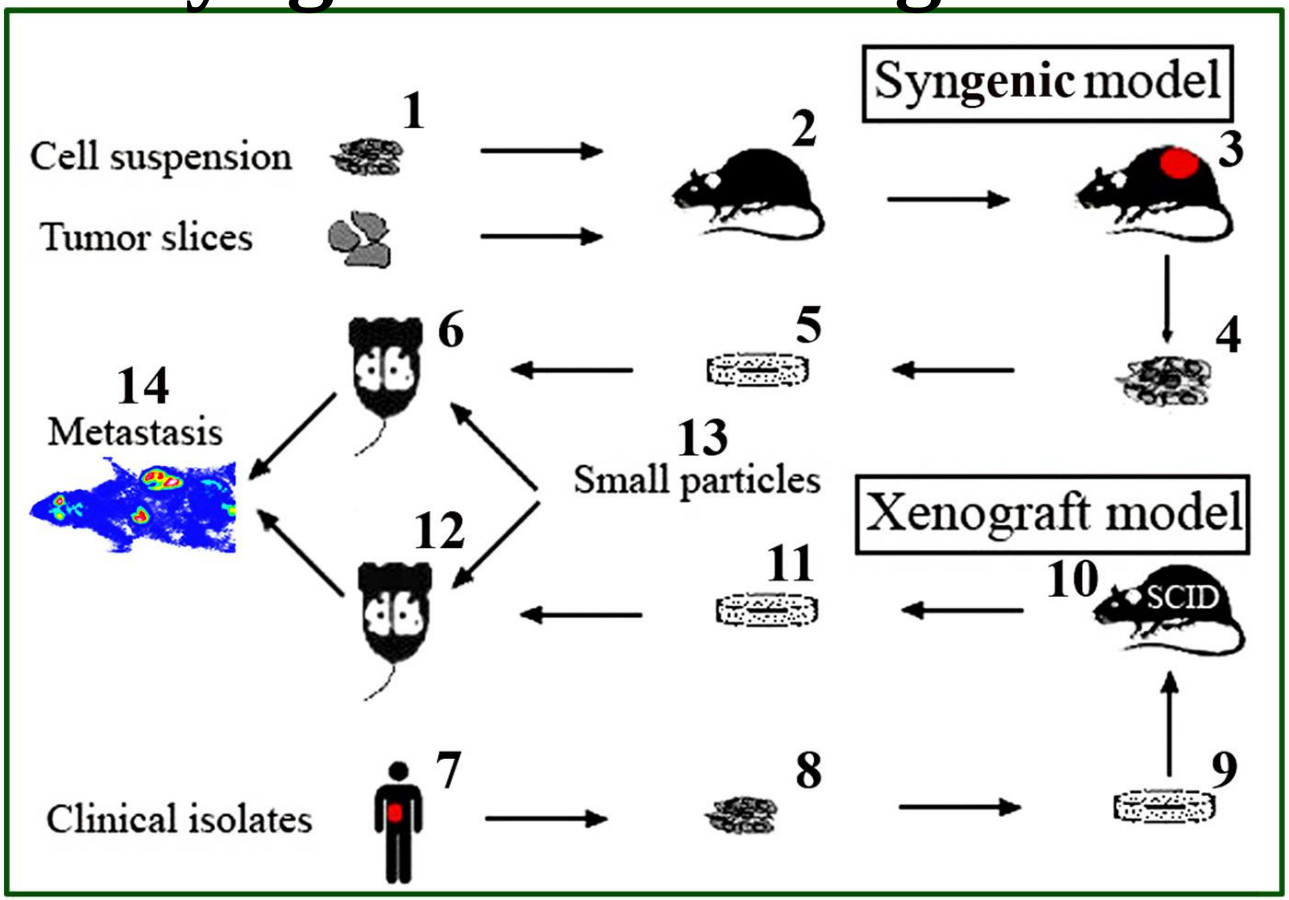

Timing of metastasis formation :

Implanted HeDe cells	Metastatic death (weeks)
10^6 cells	3
10^5 cells	4
10^4 cells	5
10^3 cells	~6

In model experiments we have used healthy mice and mice suffering in Severe Combined Immuno-deficiency (SCID) characterized by the inability to sustain an appropriate immune response against the tumor cell lines implanted. Tumor cell lines obtained from human tumors (liver, spleen, lung, kidney): implanted under the kidney capsule. Due to the absence of T and B lymphocytes tumor cells grow in SCID mice. Nanoparticles carrying the specific antitumor agent will be targeted to the sites of tumor growth. The comparison of syngenic model with the xenograft model in itself is expected to reveal the advantage of the presence of lymphocytes in supporting chemotherapy

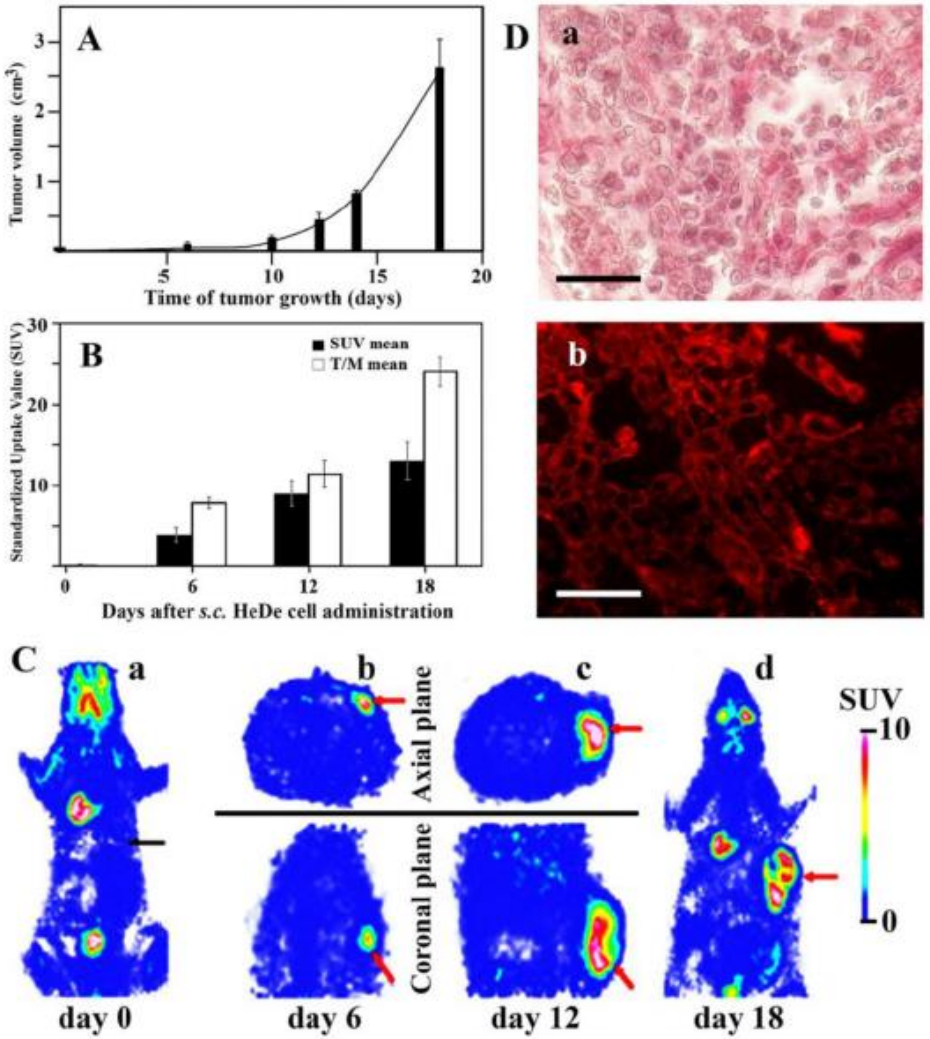

Local tumor formation upon administration of tumor cells by:

- subcutaneous (*s.c.*) injection

Trencsenyi G, Marian T, Bako F, Emri M, Nagy G, Kertai P, Banfalvi G. Metastatic hepatocarcinoma He/De tumor model in rat. J. Cancer. 5(7), 548-558 (2014).

Figure 1. Tumor formation and histological staining after s.c. administration of He/De cells. A. Growth kinetics of local tumor formation (n=3). B. ^{18}FDG-SUV mean values of subcutaneously growing primary tumors. For the estimation of T/M mean the ratio of tumor SUV mean versus background muscle SUV mean were used (n=3). C. Visualization of tumor formation by ^{18}FDG-MiniPET camera in Fischer 344 rat. a) ^{18}FDG-PET image before administration of He/De cells. Black arrow is pointing to the site of injection of He/De cells. b, c, d). Red arrows show the growing tumor at the site of injection after 6, 12 and 18 days. The Standardized Uptake Value (SUV) of ^{18}FDG was used in PET imaging as a simple semi-quantitative analysis [26]. SUV represents the ratio of the actual radioactivity concentration found in a selected part of the body at a certain time point, and the radioactivity concentration in the hypothetical case of an even distribution of the injected radioactivity across the whole body. D. Histological staining of subcutaneously growing hepatocellular He/De carcinoma. Panel a) Hematoxilin-eosin staining of subcutaneously growing hepatocellular He/De carcinoma 18 days after tumor cell implantation. Panel b) Immunofluorescent staining of subcutaneously growing hepatocellular He/De carcinoma tumor with GLUT-1 transporter and Texas red background staining. Bar: 50 μm, each.

Local tumor growth:

intravenous (*i.v.*) administration

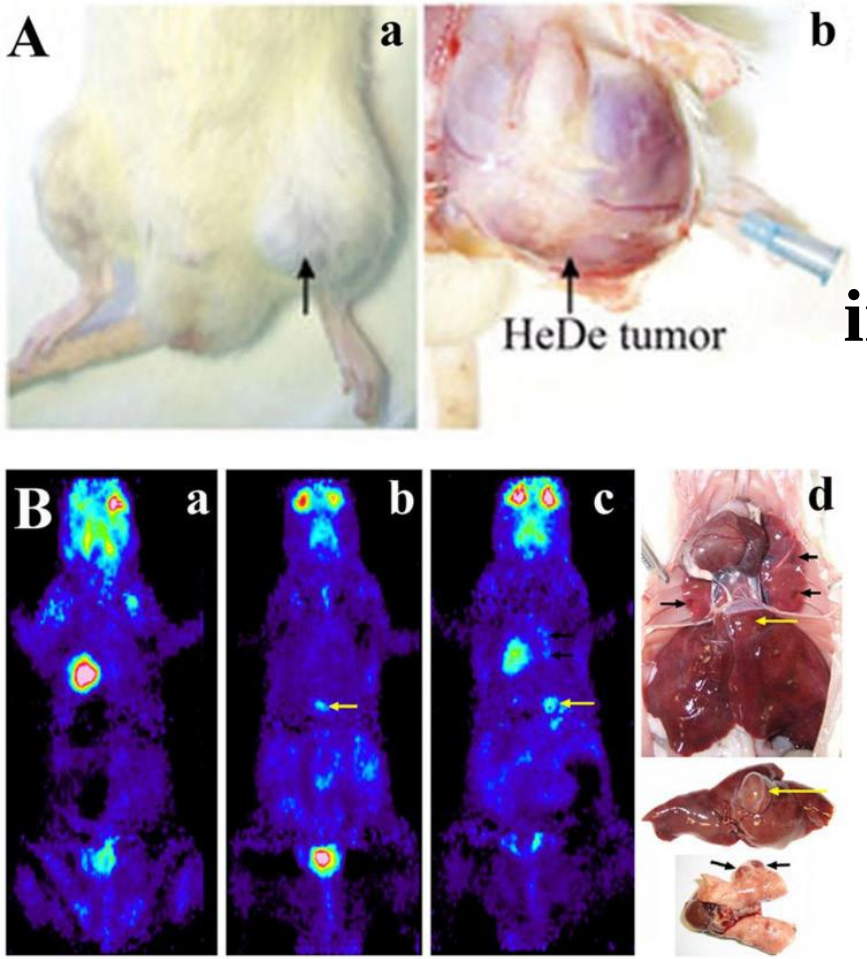

Tumor formation in rat upon injecting He/De cells in the femoral vein

A Local tumor formation. a) Tumor formation seen at the site of femoral vein injection. b) Surgical visualization of local tumor formation at the site of *i.v.* injection. Black arrows indicate the He/De primary tumor at the left hind leg. The tip of the blue needle shows the site of injection. **B.** ^{18}FDG-PET photographs taken after *i.v.* injection in Fischer 344 rats and *post mortem* examinations. a) Control: ^{18}FDG-PET image before the injection of He/De cells. b) ^{18}FDG-PET image 18 days and c) 20 days after intravenal application of He/De tumor cells. d) Tumorous lesions in the lung (black arrows), tumor formation in the liver (yellow arrows) 24 days after tumor cell administration. **C.** He/De tumor cells infiltrated in the liver 24 days after He/De *i.v.* administration. a) Hematoxilin-eosin staining. Yellow arrow points to the healthy liver tissue, black arrows are directed towards the invasion of tumor cells with large disruptions outside and inside the tumor. b) Visualization GLUT-1 transporters in liver tumor stained with Texas red. Bars: 50 μm, each.

Trencsenyi G, Marian T, Bako F, Emri M, Nagy G, Kertai P, Banfalvi G. Metastatic hepatocarcinoma He/De tumor model in rat. J. Cancer. 5(7), 548-558 (2014).

Subrenal rat implantation model

He/De, Ne/De, Me/De, My1/De, My2/De

hepatocarcinoma, nephroblastoma, melanoma , myeloid leukemia, myeloid leukemia

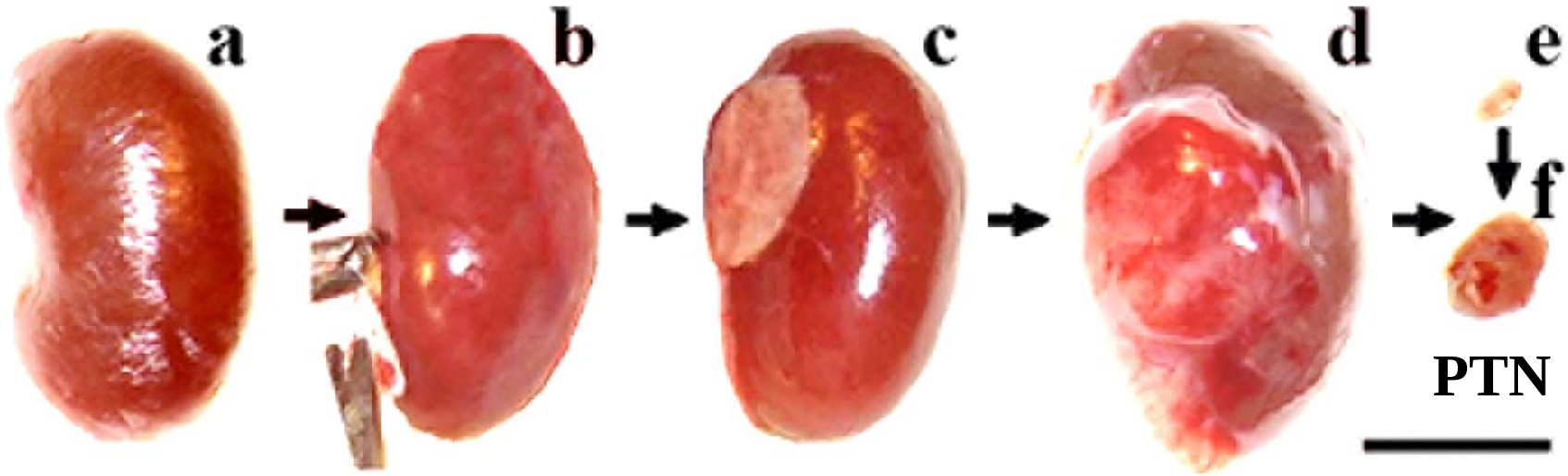

Trencsenyi G, Nagy G, Kahlik B, Kertai P, Kiss A, Banfalvi G. Lymphoid metastasis of rat My2/De leukemia. Leukemia Res. 38, 586-593 (2014).

Tissue distribution of radioactivity after *i.v.* administration of ^{18}FDG in Ne/De or He/De tumor-bearing rats

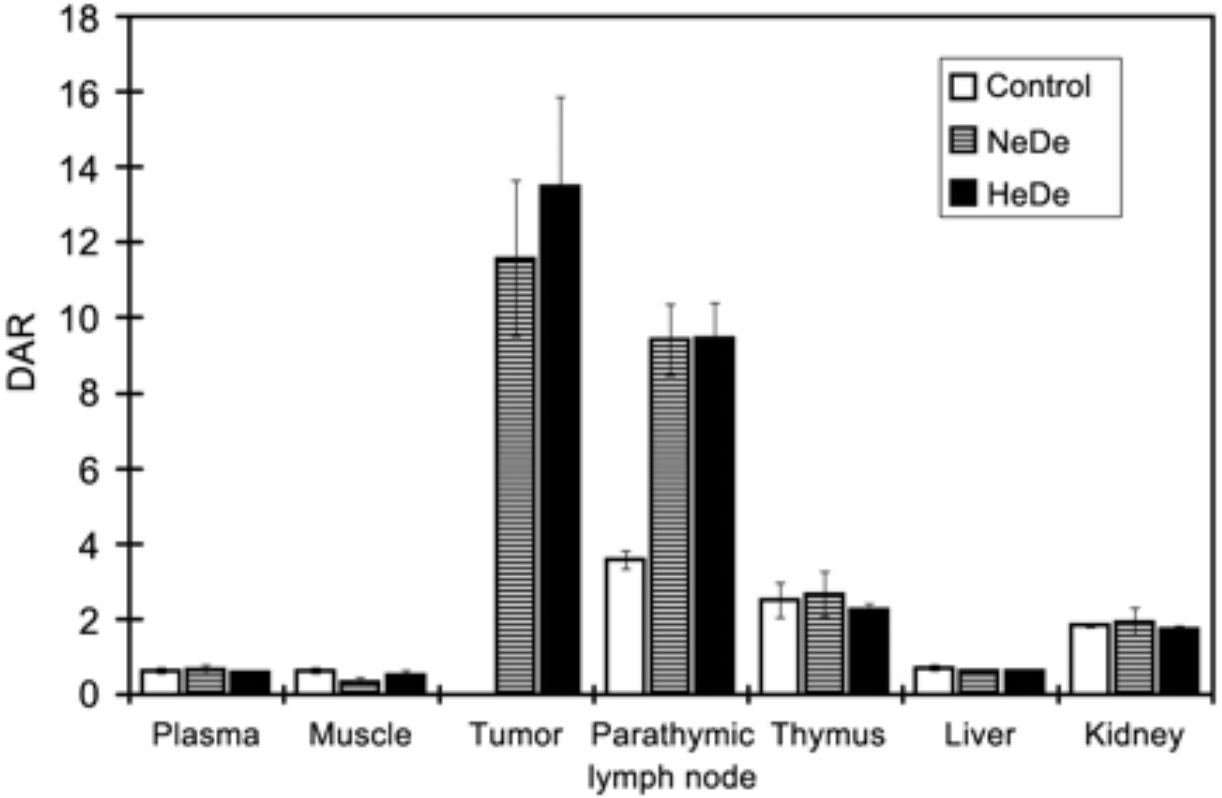

Metabolism:

-high in primary tumors and
- in PTNs

-low in other tissues

Metastatic potential of Ne/De and He/De cells, plasma, muscle, tumor, parathymic lymph nodes, thymus, liver and kidney expressed as DAR (differential absorption ratio).

Trencsenyi G., Kertai P., Bako F., Hunyadi J.,Marian T., Hargitai Z., Pocsi I., Muranyi E., Hornyak L. and Banfalvi G. Renal capsule - Parathymic lymph node complex: A new i*n vivo* metastatic model in rats. Anticancer Res. 29(6):2121-2126 (2009)

Tissue distribution of ^{18}FDG in the inner and outer part of the tumor

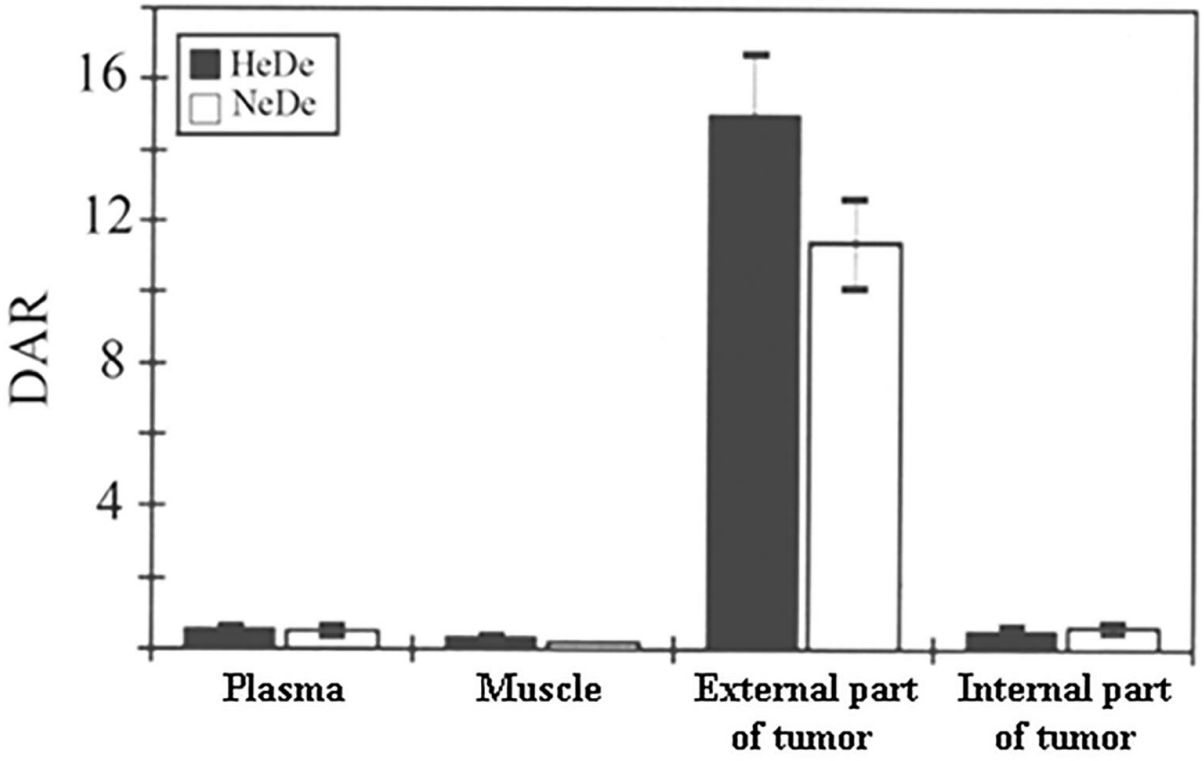

Metabolism:

-high in external part of primary tumors

-low at inner part of tumors

Outward tumor growth and inward necrosis of HeDe and NeDe tumors expressed as DAR (differential absorption ratio).

Trencsenyi G., Kertai P., Bako F., Hunyadi J.,Marian T., Hargitai Z., Pocsi I., Muranyi E., Hornyak L. and Banfalvi G. Renal capsule - Parathymic lymph node complex: A new i*n vivo* metastatic model in rats. Anticancer Res. 29(6):2121-2126 (2009)

Subrenal implantation of tumor cells

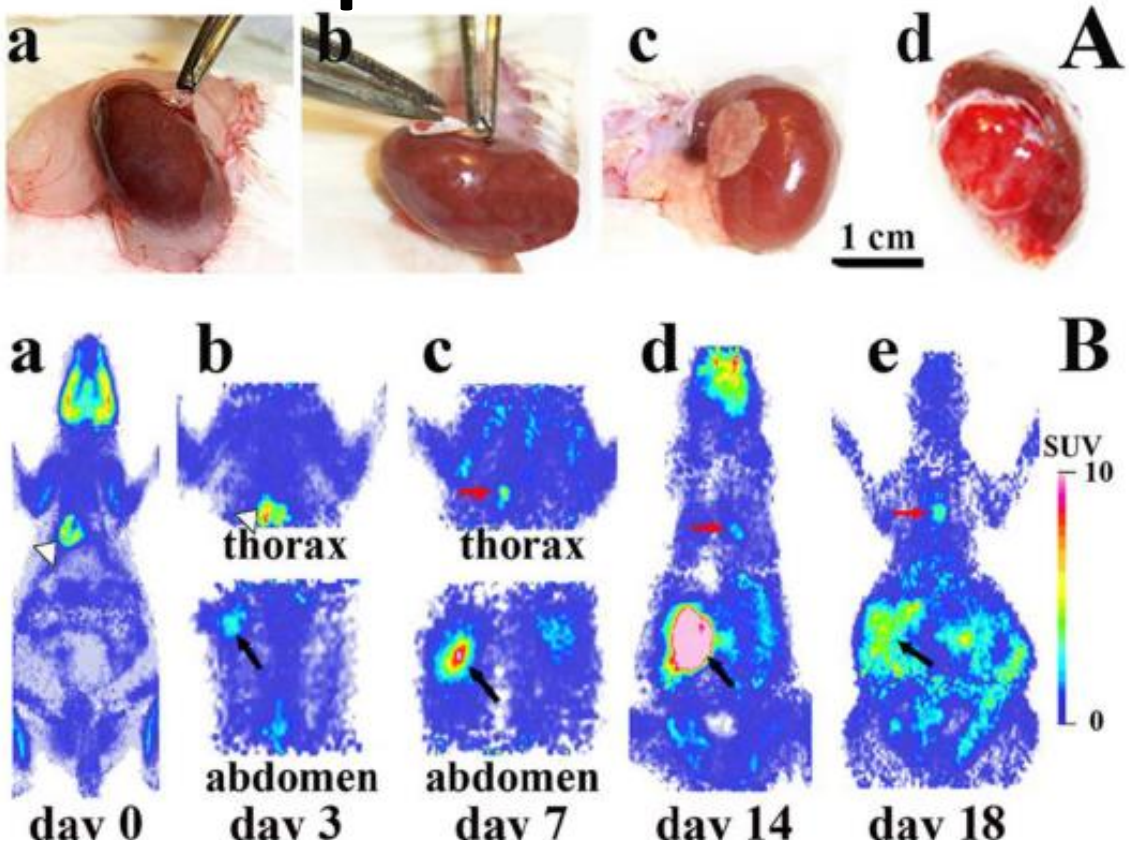

Figure 3 Tumor growth after subrenal implantatation of He/De cells. A. During the experimental surgery technique known as Subrenal Capsule Assay (SRCA): a) the left kidney of the rat was exposed, b) Gelasponge® disc containing 10^6 He/De cells was placed under the capsule of kidney, c) kidney containing the implanted tumor cells was placed back in the retroperitoneum and the operative field was subjected to post-operative treatment, d) primary tumor formation 7 days after He/De cell implantation. B. Sagittal images of ^{18}FDG-PET before and after implantation of He/De cells under the capsule of left kidney of rats. a) miniPET image before He/De cell implantation. PET images 3 days (b), 7days (c), 14 days (d) and 18 days (e) after implantation. White arrows indicate the heart, black arrows the primary tumor in kidney, red arrows metastases in parathymic lymph nodes (PTNs).

Trencsenyi G, Marian T, Bako F, Emri M, Nagy G, Kertai P, Banfalvi G. Metastatic hepatocarcinoma He/De tumor model in rat. J. Cancer. 5(7), 548-558 (2014).

Lagging angiogenesis during tumor formation
(after subrenal implantation of HeDe cells)

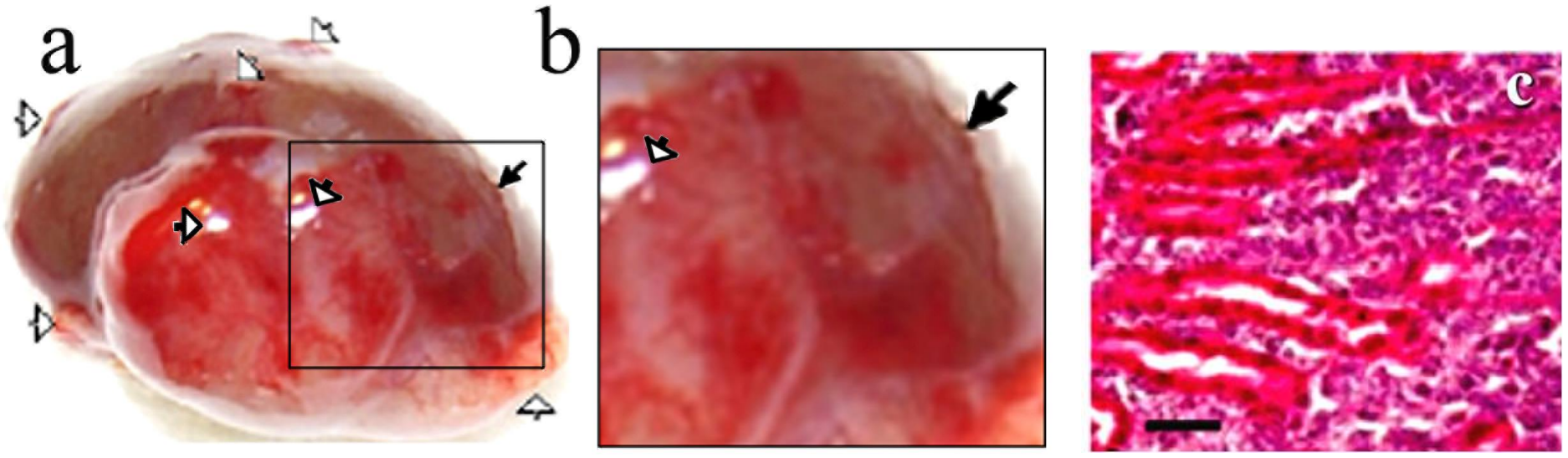

Tumor growth outward with disruption of capillaries, blood and tumor cells pour out through the disruptions.

Trencsenyi G., Kertai P., Bako F., Hunyadi J.,Marian T., Hargitai Z., Pocsi I., Muranyi E., Hornyak L. and Banfalvi G. Renal capsule - Parathymic lymph node complex: A new i*n vivo* metastatic model in rats. Anticancer Res. 29(6):2121-2126 (2009)

Subrenal implantation of nephroblastoma (NeDe) cells

Enlargement of parathymic lymph node (PTN)

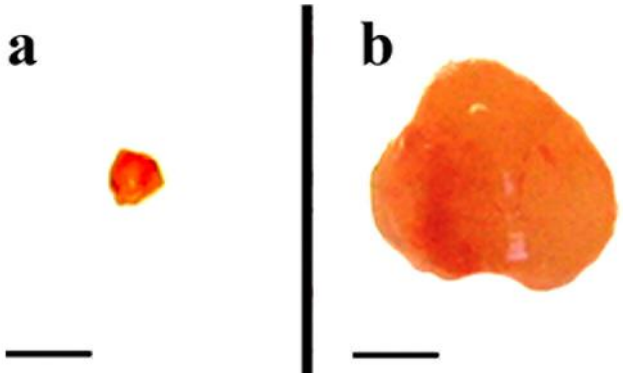

Fig. 7. Enlargement of parathymic lymph nodes six days after tumor cell implantation. a. control PTN, b. tumor-bearing PTN. Bar: 0.5 cm.

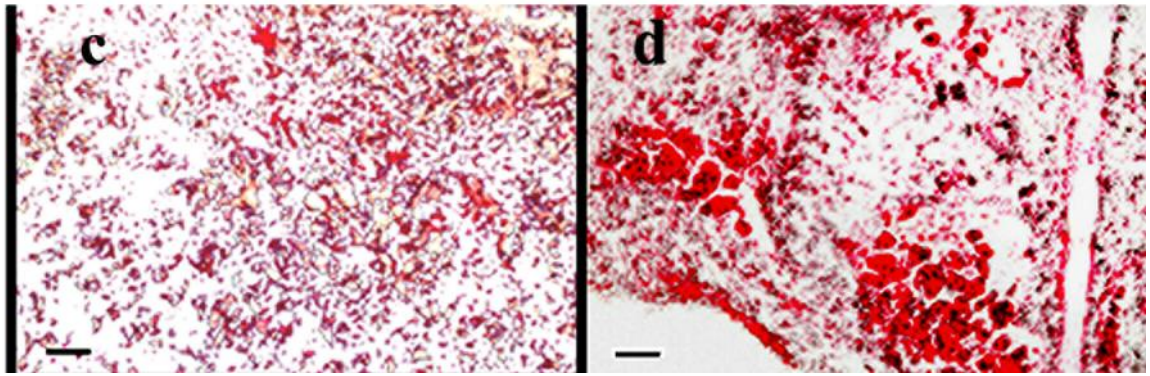

Fig. 4. Tumor infiltration in parathymic lymph nodes at day 12 after tumor cell implantation.

Rozsa D, Trencsenyi G, Kertai P, Marian T, Nagy G, **Banfalvi G.:** Lymphatic spread of mesenchymal renal tumor to metastatic parathymic lymph nodes. Histol. Histopathol. 24:1367-1379 (2009).

Lipid formation in NeDe primary tumor

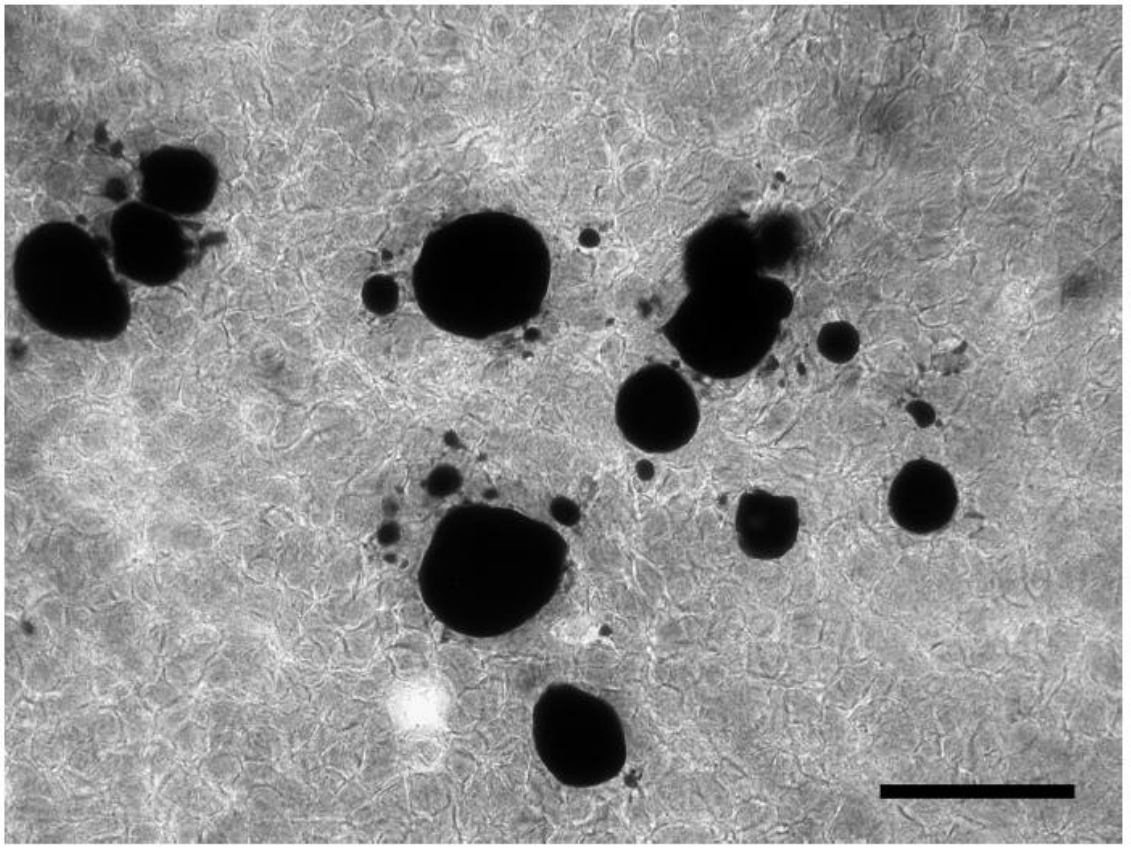

FIg. 6. Lipid droplets in primary tumor six days after tumor cell implantation. Staining: Sudan black B. Bar: 50 µm.

Rozsa D, Trencsenyi G, Kertai P, Marian T, Nagy G, Banfalvi G.: Lymphatic spread of mesenchymal renal tumor to metastatic parathymic lymph nodes. Histol. Histopathol. 24:1367-1379 (2009).

Lipogenesis in NeDe tumor

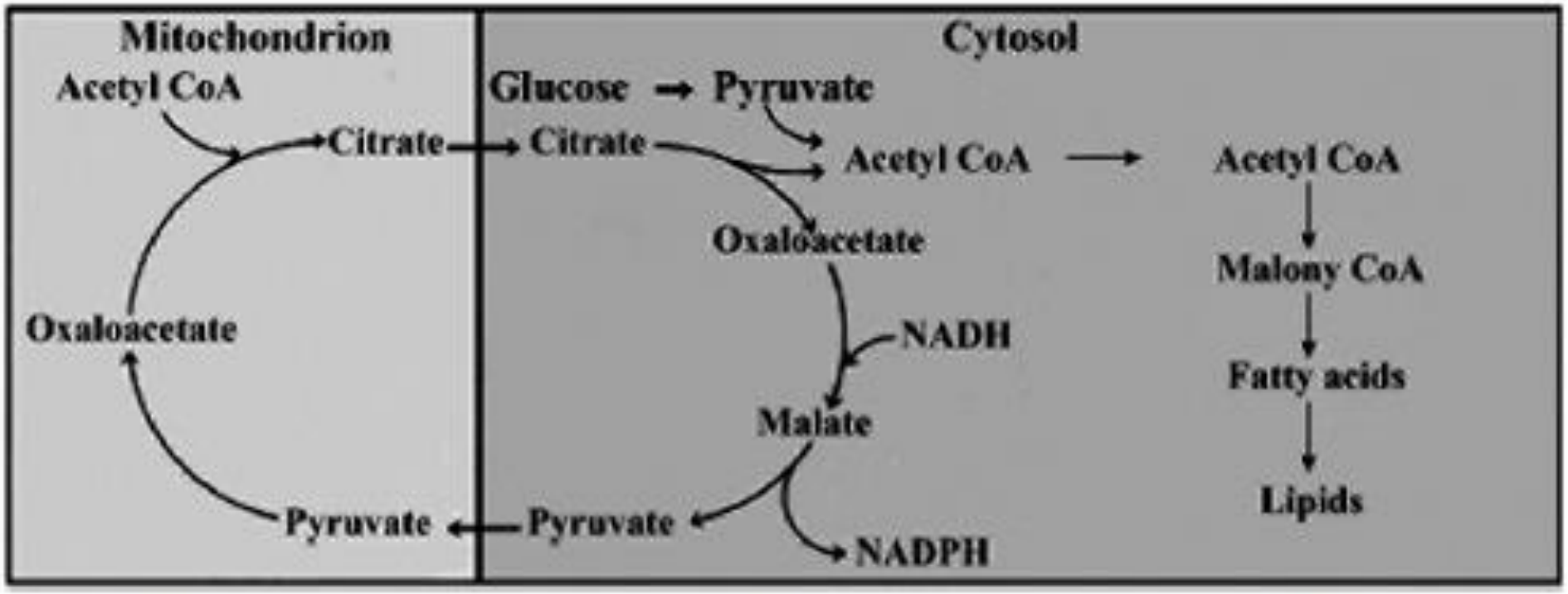

FIg. 10. Lipogenic pathway in NeDe tumor. In the mitochondria of tumor cells the terminal oxidation and the oxidative phosphorylation are not working under hypoxic conditions. In the absence of the normal aerobic metabolism the overproduction of acetylcoenzyme A induces fatty acid and lipid synthesis.

Rozsa D, Trencsenyi G, Kertai P, Marian T, Nagy G, Banfalvi G.: Lymphatic spread of mesenchymal renal tumor to metastatic parathymic lymph nodes. Histol. Histopathol. 24:1367-1379 (2009).

Metastasis in parathymic lymph nodes caused by nephroblastoma (NeDe) cell implantation

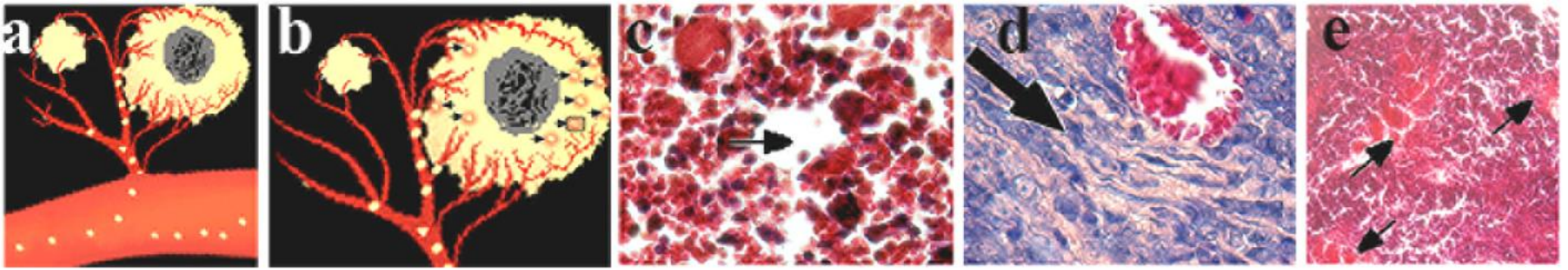

a) Elevated peripheral pressure in abdominal kidney tumor
b) produces an increased amount of fluid accumulating in the peritoneal cavity.
(Uroperitoneum subsequent to kidney, ureter, bladder, or urethra rupture also cause an increased amount of effusion in the abdomen. Pleural neoplastic effusions are known to occur frequently (Ultmann JE: *CA: Cancer J Clin* 1962,**12**:42–50).

c and d) Rat mesenchymal renal tumor cells (Ne/De) transplanted under the kidney capsule of F344 rats pour through the disruptions of blood vessels into the retroperitoneum and
d) cross the diaphragm and appear in the PTNs

Rozsa D, Trencsenyi G, Kertai P, Marian T, Nagy G, Banfalvi G.: Lymphatic spread of mesenchymal renal tumor to metastatic parathymic lymph nodes. Histol. Histopathol. 24:1367-1379 (2009).

Mimicking metastatic spread by India ink implantation in rats

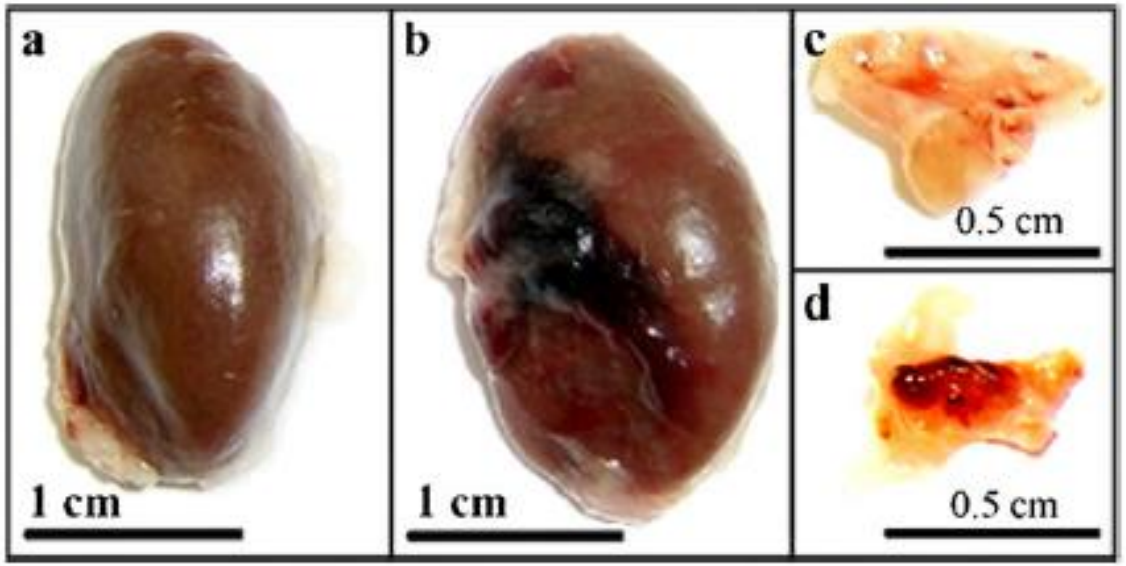

Fig. 2 Demonstration of tumor spread by the implantation of colloidal India ink and its appearance in PTNs. **a** Normal kidney of rat. **b** Implantation of India ink under the renal capsule. **c** Normal parathymic lymph nodes. **d** Accumulation of India ink in PTNs 6 h after implantation. Modified with permission [41]

Banfalvi G. Metastatic view of breast cancer. Cancer Metast. Rev. 31:815–822 (2012)

Spread of metastasis

from organs to other organs primarily to the liver (well known)

from abdominal (peritoneal, retroperitoneal) tumors to parathymic lymph nodes (not well understood)

Organ	Primary tumor	Metastasis
Brain		central nervous system
Breast		bone, lung, liver, brain
Lung		liver, bone, brain, adrenal gland
Liver		**not specified**
Colon		liver, lung, peritoneum
Kidney		liver, lung, bone, brain
Bone		lung, other bones
Ovary	Ovaries	liver, lung, peritoneum
Prostate		bone, lymph nodes, liver, lung

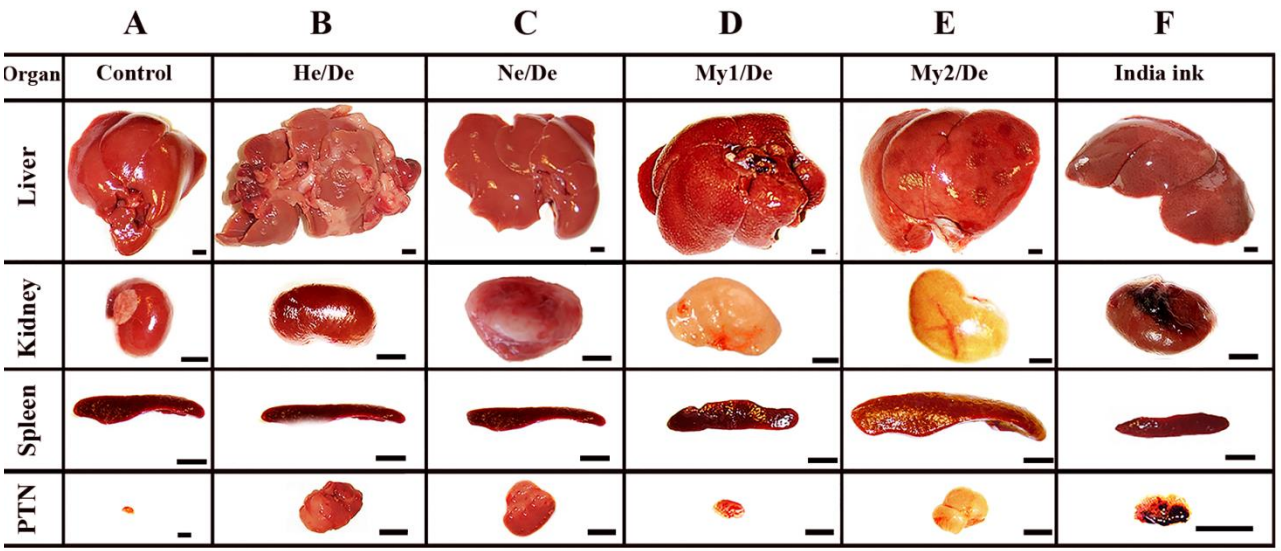

Metastasis: abdominal primary tumor → thoracal (PTN)

↓ mammary lymph nodes

Metastatic spread of primary tumor to thoracal and parathymic lymph nodes in rat

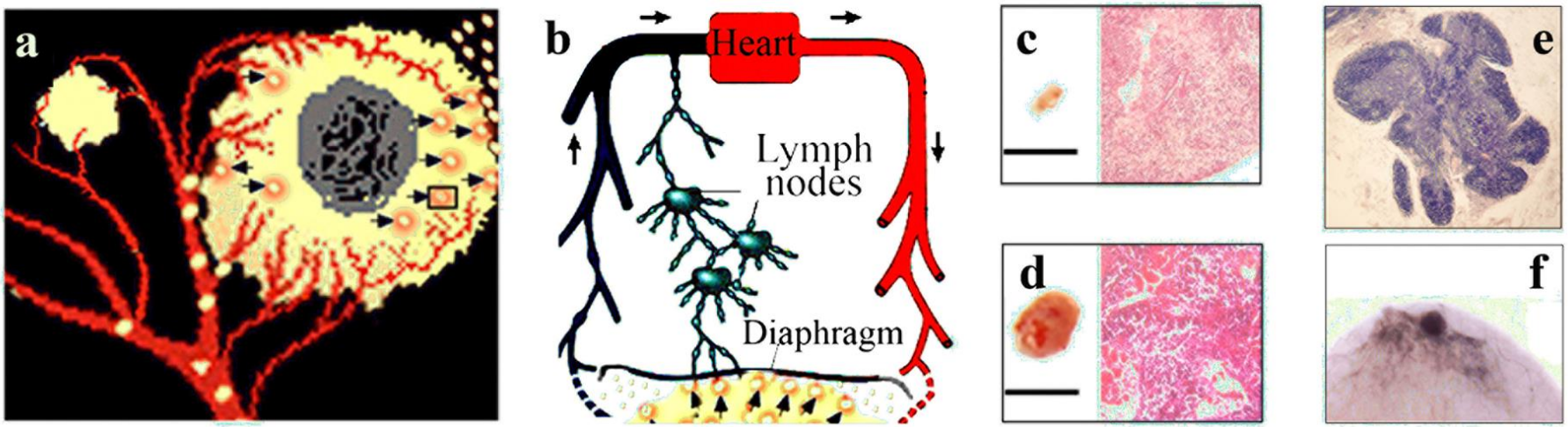

Banfalvi G. Role of parathymic lymph nodes in metastatic tumor development. Cancer Metastasis Rev (2012) 31:89–97.

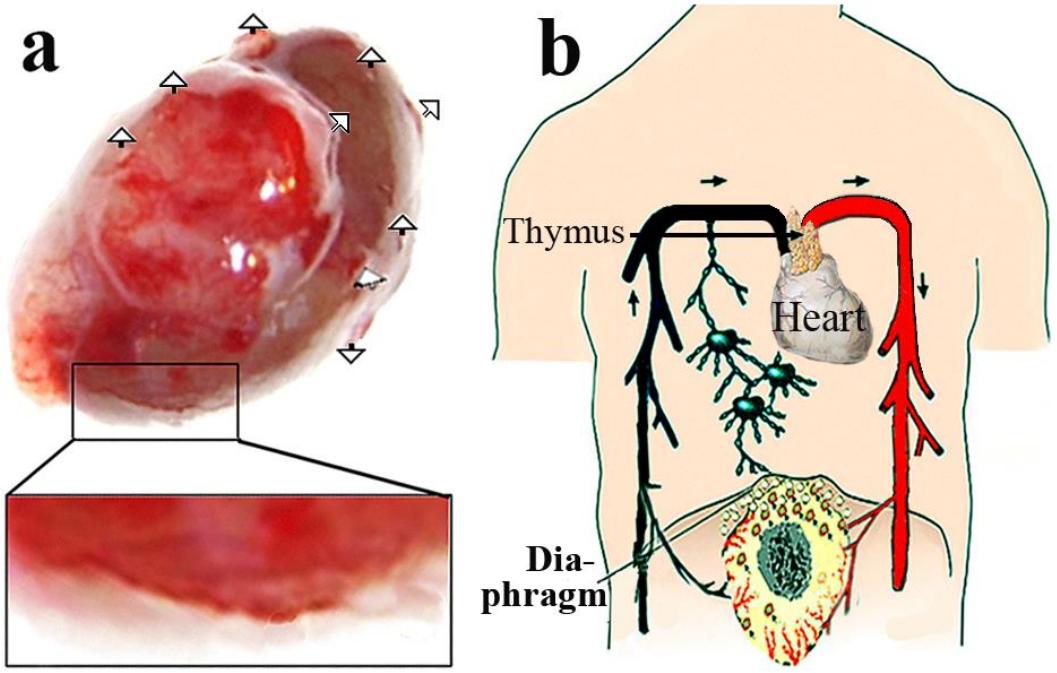

Similar human metastatic spread of abdominal tumors to inner mammary lymph nodes

i) Disruptions in the abdominal primary tumor (arrows in **a**)

ii) Release of tumor cells through gastrointestinal bleeding of the primary tumor and their appearance in the abdominal space (**a**)

iii) Migration of tumor cells by pass the hiatuses of the diaphragm (**b**)

iv) Tumor cells exhaust the defense capacity of the parathymic organ

v) Unchecked tumor cells migrate from the inferior to the superior thoracal lymph nodes and drain to the vascular system (**b**).

Banfalvi G. Role of parathymic lymph nodes in metastatic tumor development. Cancer Metast. Rev. 31(1-2): 89-97 (2012).

Anatomical illustration of lymph nodes in the thoracic region

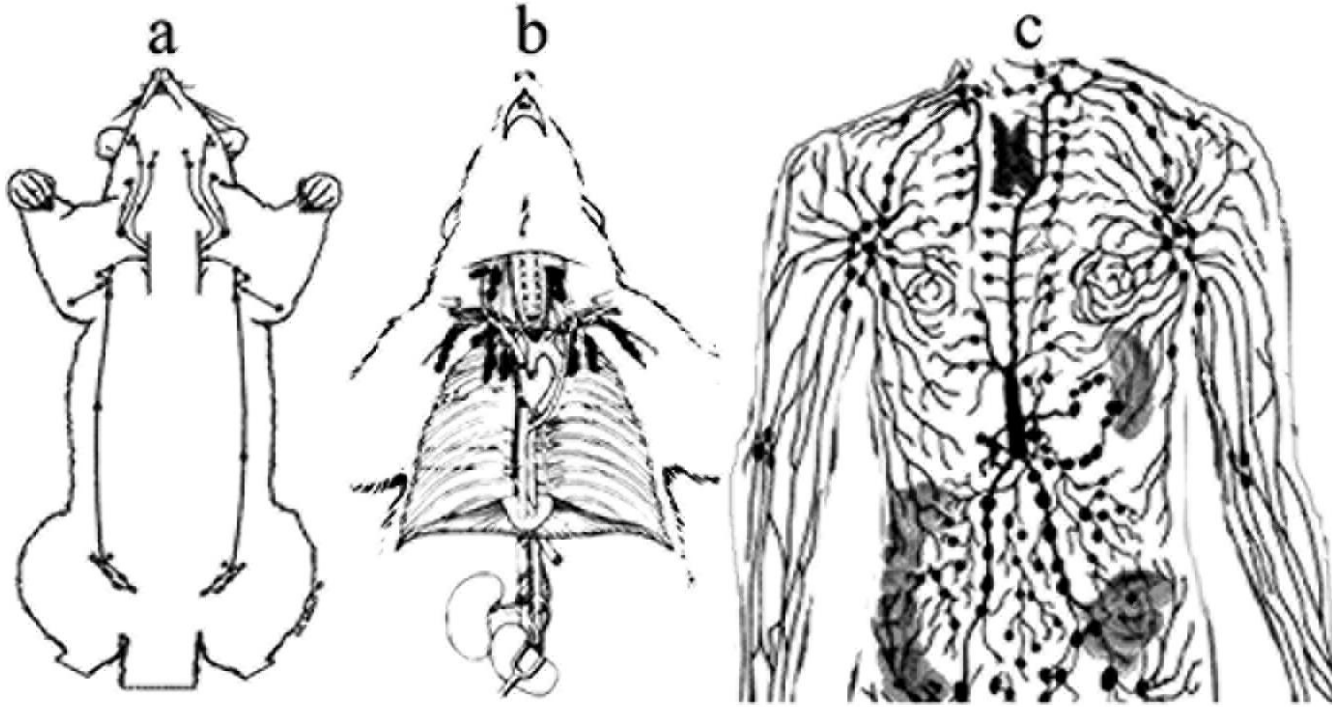

Opossum **Rat** **Human**

Fig. 3 Anatomical illustrations of lymph nodes in the thoracic region. **a** The low number and small size of thoracic lymph nodes explain why opossums are inefficient against tuberculosis. **b** The lymphatic system of rats is resistant to tubercle bacilli. **c** The lymphatic system of the human thorax is more resistant to tuberculosis than marsupials, but less developed than those of rodents. Connections among thoracic and mammary lymph nodes are poorly understood

Banfalvi G. Metastatic view of breast cancer. Cancer Metast. Rev. 31:815–822 (2012)

Metastatic spread of abdominal tumors to mammary lymph nodes

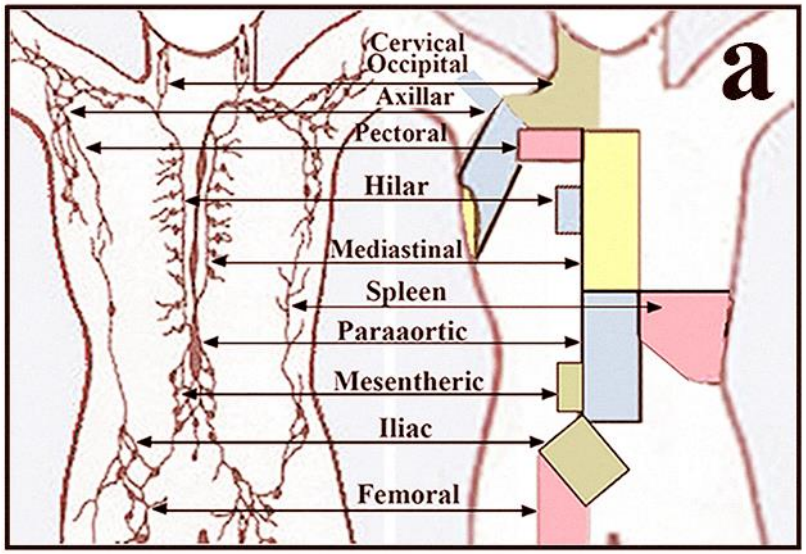

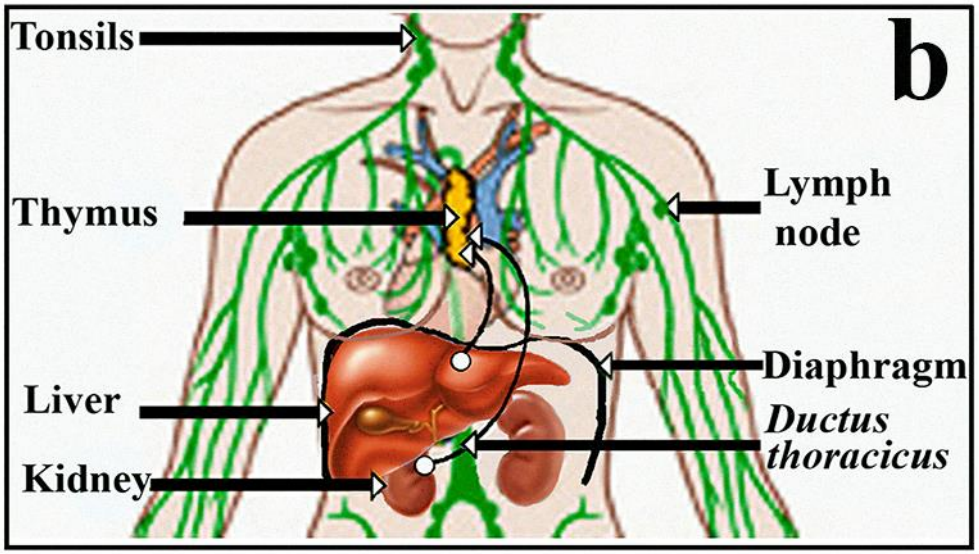

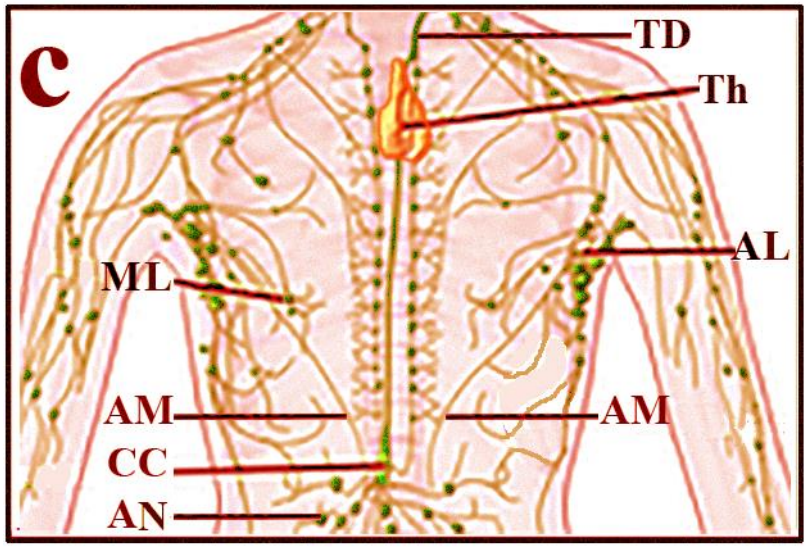

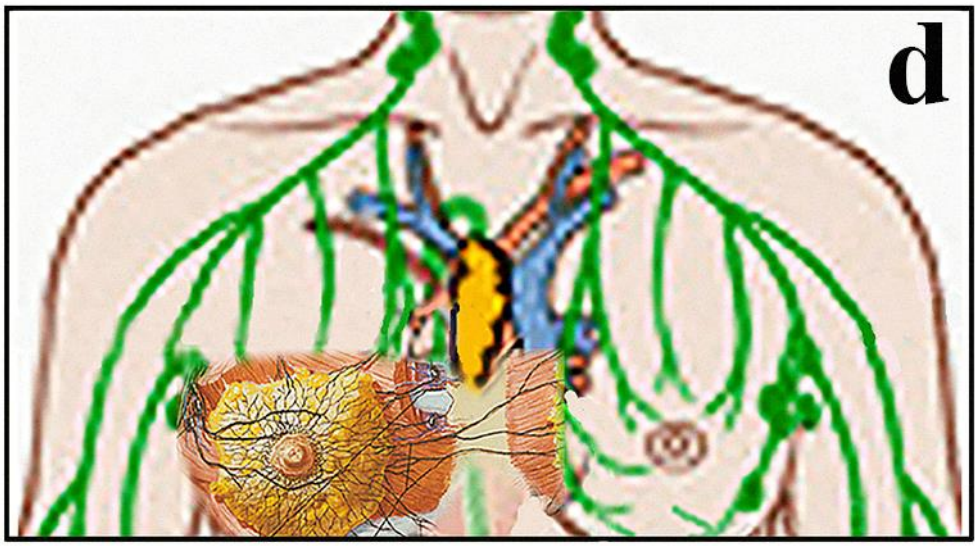

Banfalvi G. Metastatic view of breast cancer. Cancer Metast. Rev. 31:815–822 (2012)

What did others find?

- High radiotracer glucose analogue uptake in PTNs is in correlation with the inflammatory activity in the liver (1).
- After intraperitoneal administration of oncolytic measles virus-infected cells, the diaphragmatic stomata, thoracic lymphatic vessels, and parathymic lymph nodes contained numerous measles-infected cells (2).
- 9–45% axillary lymph node tumors drain to the internal mammary lymph nodes (IMLN) (3-6).
- In almost all patients the internal mammary lymph node tumor is a forerunner of a metastatic disease (7).
- Handley and Thackray concluded that the internal mammary glands may often be invaded before carcinoma has reached the axilla . Their clinical evidence indicates a relatively high incidence (~ 25%) of scondary spread to the breast (8).
- There is a direct anatomical connection between abdominal and mammary lymph nodes (9).

1. Friedrich-Rust et al. *Am J Roentgenol* 2007,**188**:758-764.
2. Peng et al. *Human Gene Ther* 2003,**14**:1565-1577
3. Uren et al. *World J Surg* 2001, **25**:789-793.
4. Bird et al. *Ann Surg Oncol* 2001, **8**:234-240.
5. van der Ent et al. *Ann Surg* 2001, **234**:79-84.
6. Lamonica et al. *Clin Nucl Med* 2003, **28**:558-64.
7. Cranenbroek et al. *Breat Cancer Treat* 2005, **89**:271-275.
8. Handley and Thackray *Brit J Cancer* 1947, **1**:15–20.
9. Gray Anatomy(1901 edn).

Summary

The migration of abdominal tumor cells can be summarized as:

i) implanted tumor cells cause primary tumors and peripheral disruptions of primary tumors,
ii) tumor cells are shedded into the abdominal cavity,
iii) released tumor cells cross the stomata of the diaphragm,
iv) tumor cells accumulate in thoracal, primarily in parathymic (rodent), inner mammary (human) lymph nodes,
v) after exhausting the defense capacity of parathymic lymph nodes, metastatic migration continues in the superior lymph node chain before the thoracic duct returns chyle to the vascular system,
vi) colloidal carbon particles mimic faithfully the migration of tumor cells.

Conclusions

- The study of abdominal tumor spread to mammary lymph nodes has been neglected earlier due to the belief that mammary tumors are not metastases.
- The metastatic spread of tumor cells released from abdominal primary tumors to PTNs was found by using different cell lines including solid rat liver (He/De), kidney (Ne/De) and leukemia (My1/De, My2/De) cell lines.
- Why human parathymic lymph nodes have not been investigated earlier ? Answer: they were investigated but were known as inner mammary lymph nodes (not to be confused with intra-mammary lymph nodes).
- The significance of potential spread of metastasis from the most often occuring abdominal primary tumors to mammary lymph nodes is emphasized. The spread of abdominal tumors cells to mammary lymph nodes provides a new explanation to the origin of breast metastasis and alternative for prevention.

For more information see:

Banfalvi G. Homeostasis – Tumor – Metastasis . Springer, New York, 2013. ISBN 978-94-007-7334-9

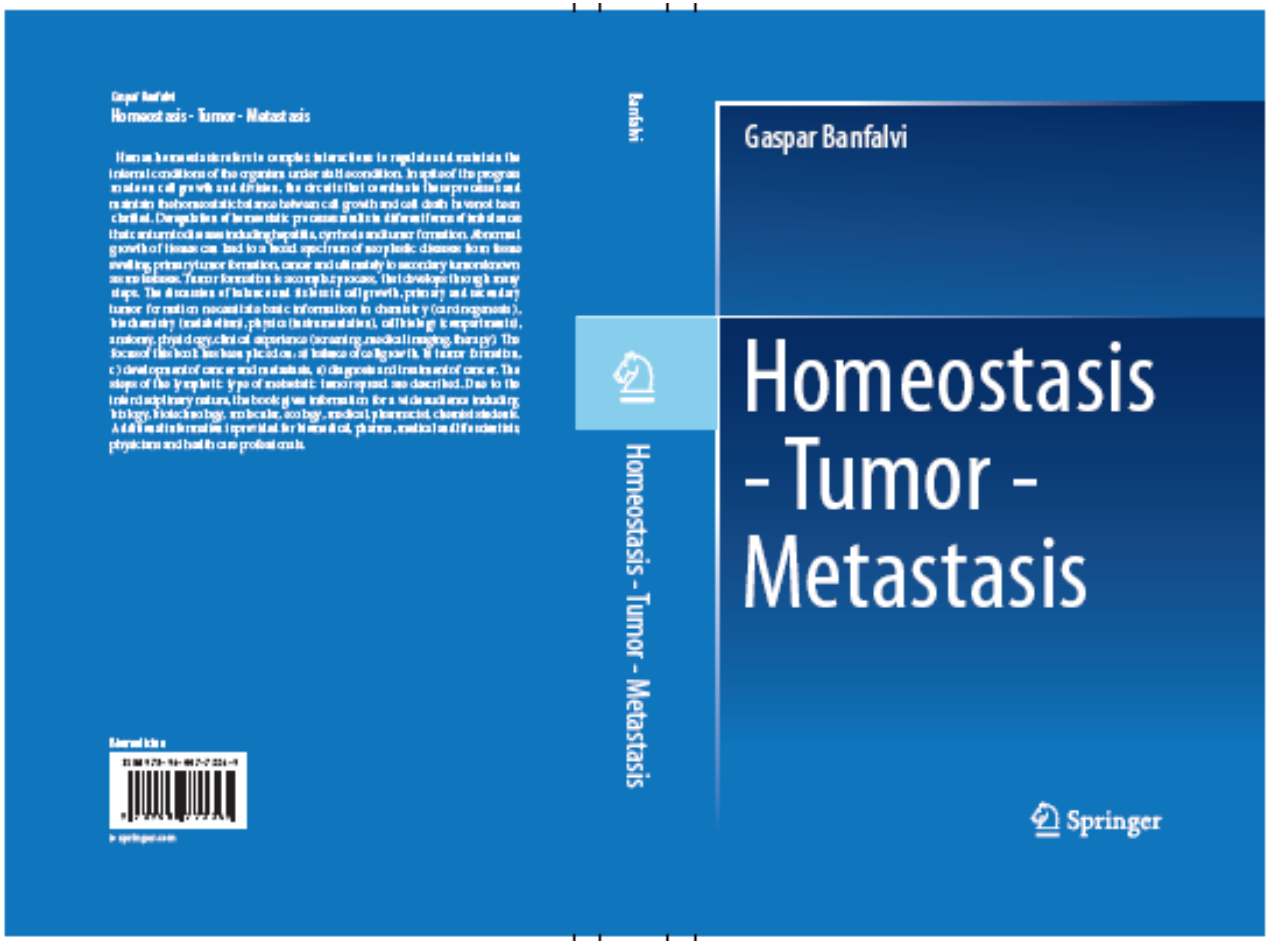

http://link.springer.com/book/10.1007/978-94-007-7335-6/page/1

Gmail: gaspar.banfalvi@gmail.com

Acknowledgements to

Students:

- Nagy, Gábor PhD
- Trencsényi ,György PhD
- Rőszer ,Tamá,s, PhD Ulm
- Ujvárosi , Kinga, PhD
- Pintér ,Gábor
- Gácsi, Mariann PhD
- Szepessy, Edit PhD, MD
- Buzder ,Tímea PhD
- Rehak Marian PhD

Technical contribution:

- Somogyi, Csilla
- Farkas, Erzsébet
- Laza, Diána
- Sárvári, Anitta
- Bakó, Fruzsina
- Balogh, Enikő
- Pócsi, Imre
- Turáni ,Melinda
- Tánczos, Bence
- Király, Gábor
- Tálas, László
- Pinczés, Gyula
- Kukoricza, Krisztina
- Jákim, Judit
- Fidrus, Eszter
- Vörös, Orsolya

Professors:

- Kertai, Pál, DE
- Hunyadi, János, DE
- Alexei Basnakian, Little Rock
- Németh, Péter, Pécs
- Varda Rotter, Weizmann Intézet
- Henry Paulus, Harvard
- Hans Tanke, Leiden
- † Tuneko Okazaki, Nagoya
- † Edward Wood, Leeds
- Pócsi, István, head of department

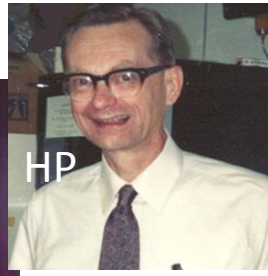

Thank you for your attention!